Journal of
Ceramic Science
and Technology

J. Ceram. Sci. Tech., **06** [04] 305-314 (2015)
DOI: 10.4416/JCST2015-00053
available online at: http://www.ceramic-science.com

Small-Size Low-Loss Bandpass Filters on Substrate-Integrated Waveguide Capacitively Loaded Cavities Embedded in Low Temperature Co-Fired Ceramics

V. Turgaliev[1], D. Kholodnyak*[1], J. Müller[2], and M.A. Hein[2]

[1]St Petersburg Electrotechnical University "LETI", 5 Prof. Popov Str., 197376 St Petersburg, Russia
[2]Ilmenau University of Technology, 98693 Ilmenau, Germany

received September 1, 2015; received in revised form October 26, 2015; accepted November 13, 2015

Abstract

The design of microwave filters for portable electronics is complicated by conflicting requirements that must be met simultaneously such as high selectivity, low insertion loss and compact size. Substrate-integrated waveguide (SIW) technology allows the design of low-profile high-Q resonators and low-loss filters based on this. However, SIW filters are not well suited for telecommunication applications because of their remarkably large size in plane. The size of a SIW cavity can be dramatically reduced with the use of capacitive loading. Capacitively loaded cavities (CLCs) operating in the TM_{110} mode are shown to be as small as 1/8 of the guided wavelength and even smaller, i.e. comparable in size with lumped-element resonators. Although the unloaded Q-factor decreases proportionally to cavity size, miniaturized CLCs can exhibit a much higher Q-factor than that of lumped-element resonators. This paves the way for designing small-size and low-loss filters for wireless communications and different applications. Miniaturized capacitively loaded SIW cavities are favorably implemented by means of low-temperature co-fired ceramics (LTCC) technology. The goal of the paper is to demonstrate the manifold possibilities and flexibility offered by LTCC technology for the design of advanced microwave filters on CLCs. Different design and manufacturing aspects are considered. Various design examples of high-performance LTCC resonators and filters for single- and dual-band wireless applications are presented. The designed resonators and filters were manufactured using the commercial DuPont Green Tape 951 LTCC system. The LTCC filters on miniaturized CLCs are shown to be advantageous with regard to small size, low loss, and absence of spurious response over a wide frequency range.

Keywords: Substrate-integrated waveguide (SIW), low temperature co-fired ceramics (LTCC), capacitively loaded cavities, dual-mode resonators, bandpass filters.

I. Introduction

Microwave filters are indispensable front-end components of all manner of telecommunication and wireless systems. Filters for the future generation of portable wireless electronics have to be compact, lightweight and cheap while exhibiting high selectivity and low insertion loss. Such conflicting requirements that must be met simultaneously complicate filter design considerably. Advanced small-size resonators with a high quality factor are required to overcome the problem.

The in-band insertion loss of a bandpass filter (*IL*) depends on the fractional bandwidth ($\Delta f/f_0$), the unloaded quality factor of resonators (Q_U) and the filter order (the number of resonators involved – *N*). The minimum insertion loss that is provided at the midband frequency f_0 can be roughly evaluated as follows

$$\mathrm{IL}(f_0) \approx 4.343 \frac{\mathrm{N}}{\mathrm{Q_U}\Delta f/f_0} \qquad (1).$$

According to (1), a high resonator Q-factor is required to realize a low-loss narrowband filter. In turn, a broadband filter of the same order exhibits less insertion loss but provides less selectivity as well. An increase of the filter order *N* to improve the selectivity is followed by an increase of the insertion loss in line with (1). Consequently, design of either narrowband or highly selective broadband filters involves a necessity to employ high-Q resonators in order to keep the insertion loss at a tolerable level.

The unloaded Q-factor is defined as the energy stored in the resonator (*W*) related to the power loss (P_{loss}) per oscillation period:

$$\mathrm{Q_U} = \omega_0 \mathrm{W}/\mathrm{P_{loss}} \qquad (2),$$

where $\omega_0 = 2\pi f_0$ is the angular midband frequency.

The unloaded Q-factor is determined by the resonator electromagnetic structure (i.e. the electric and magnetic field distribution in the resonator) as well as the conductor and dielectric losses of the materials of which the resonator is made. There is a trade-off between resonator size and Q-factor value. The smaller the resonator size compared to the guided wavelength (λ_g), the lower the unloaded Q-factor. That is why bulky and heavy waveguide and cavity filters allow quite a low insertion loss to be obtained

* Corresponding author: Dmitry.Kholodnyak@mwlab.spb.ru

whereas lumped-element filters suffer from a poor Q-factor, resulting in a remarkable insertion loss level.

The substrate-integrated waveguide (SIW) technology [1] is a beneficial alternative to conventional waveguides and cavities that allows the design of low-profile, lightweight and low-loss filters based on high-Q resonators [2–9]. SIW structures are favorably realized in printed-circuit board (PCB) technology or low-temperature co-fired ceramics (LTCC) technology.

Despite the advantages in height and weight, typical SIW filters still occupy a rather large area and consequently are not well suited for low-frequency microwave applications.

Loading a cavity with a capacitive post reduces the resonant frequency while still maintaining a relatively high unloaded Q-factor [10]. Various designs of compact microwave filters based on capacitively loaded evanescent-mode cavities using different fabrication technologies (LTCC, PCB, silicon micromachining process) have been reported [10–14].

Still, there remains a trade-off between the size and the Q-factor of capacitively loaded cavities (CLCs). The ultimate miniaturization of a cavity is accordingly limited by a Q-factor value tolerable for certain application. Compared with a high Q-factor of the unloaded cavity, there is only little room for size reduction owing to a remarkable Q-factor drop. However, with regard to lumped-element resonators, whose Q-factor is much smaller, there is plenty of headroom for downsizing while keeping the Q-factor at a tolerable level.

Miniaturized LTCC CLCs can be designed as small as lumped-element resonators (i.e. smaller than 1/8 of the guided wavelength) while exhibiting a much higher Q-factor [15,16].

The manifold possibilities and flexibility offered by multilayer LTCC technology to the design of advanced microwave filters on CLCs are discussed in this paper. Different design and manufacturing aspects are considered including single- and dual-mode CLCs implementation on LTCC, CLCs with transmission zeros to increase selectivity, inter-resonator coupling organization, band-pass filter design using CLCs, etc. Various design examples of high-performance LTCC resonators and filters for single- and dual-band wireless applications are presented.

The resonators and filters were designed with the aid of the Ansoft HFSS 3D electromagnetic field solver and manufactured using the commercial DuPont Green Tape™ 951 LTCC system.

II. LTCC capacitively loaded cavities

(1) SIW cavities in LTCC technology

Waveguide-like structures implemented in planar technology by using periodic metallic via holes as sidewalls are called substrate-integrated waveguides (SIWs) [1]. Fig. 1a shows a rectangular SIW cavity in LTCC technology. The cavity volume filled with LTCC is confined by metallic covers on the top and the bottom of the structure. Stacked metallic via holes form the conductive fences to realize sidewalls. A period of the via fences has to be much smaller than the resonant wavelength to prevent energy radiation through the sidewalls.

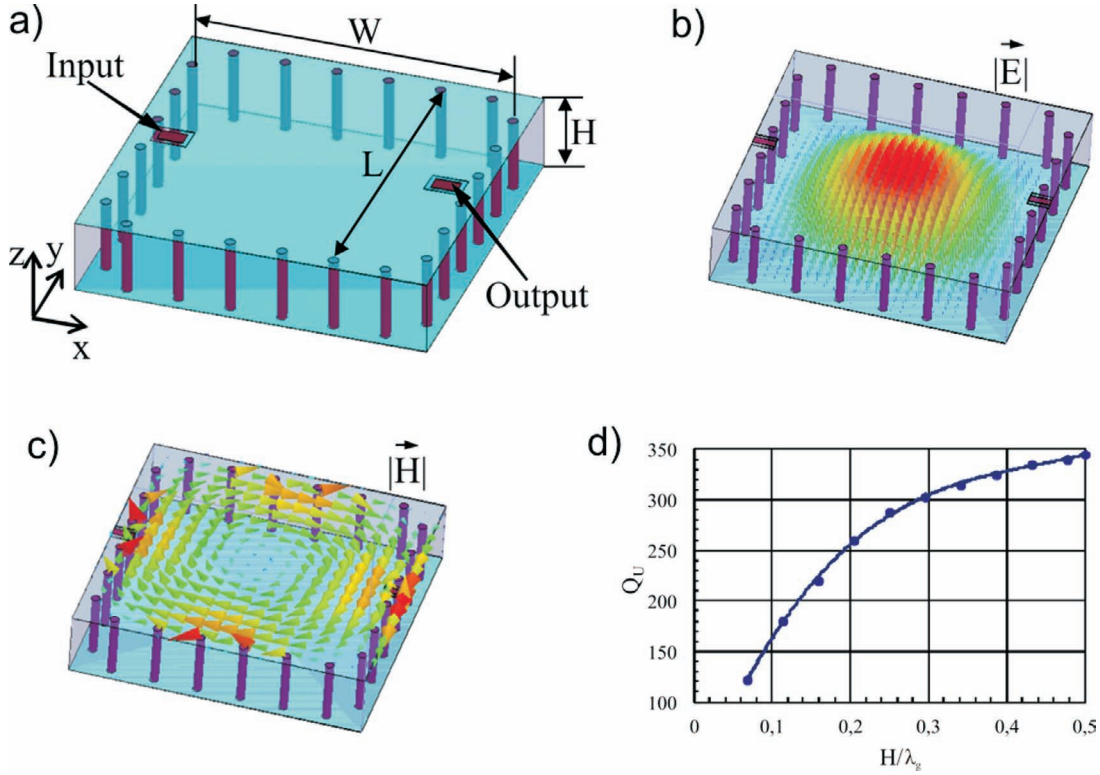

Fig. 1: Rectangular SIW cavity: (a) structure 3D view; (b) electric field distribution for the TM_{110} mode; (c) magnetic field distribution for the TM_{110} mode; (d) unloaded Q-factor of a LTCC-filled cavity as a function of the resonator height related to the guided wavelength.

Owing to planar implementation, the height H of a SIW cavity does not exceed a few millimeters. Therefore, the cavity operates in the TM_{110} mode. The coplanar feed lines used for excitation are arranged in the cavity top cover. Distribution of the electric and magnetic fields are presented in Figs. 1b and c correspondingly. The cavity resonant frequency is equal to

$$f_0 = \frac{c}{2\sqrt{\varepsilon_r}}\sqrt{\left(\frac{1}{W}\right)^2 + \left(\frac{1}{L}\right)^2} \qquad (3),$$

where c is the light velocity, ε_r is the relative permittivity of a dielectric that the cavity is filled with, W and L are the cavity sizes in plane (see Fig. 1a). Typical values of the relative dielectric permittivity of most commercial LTCC materials lie in the range 5 – 9. Besides, LTCC materials with higher ε_r values are known as well.

Although the resonant frequency of the fundamental mode does not depend on the cavity height H, the unloaded Q-factor does. The dependence obtained by electromagnetic simulations for a SIW cavity filled with the DuPont Green Tape™ 951 LTCC ($\varepsilon_r = 7.8$, $\tan\delta = 0.002$) is shown in Fig. 1d. It is worth mentioning that at a five-fold height decrease, e.g. from $0.5\lambda_g$ to $0.1\lambda_g$, the unloaded Q-factor drop is only two-fold (i.e. from 340 to 170).

(2) Capacitively loaded SIW cavities

Fig. 2a illustrates a square-shape SIW cavity ($W = L = a$) that is loaded by a conductive post with a metallic plate at one end. The post is formed by stacked metallic via holes. The middle part of the cavity top cover is not shown in the figure so as to illustrate the inner resonator structure in detail.

The electric field is concentrated between the metallic plate and the top cover (Fig. 2b). As electric energy is stored in the region, it is by nature of a capacitive loading. The higher the capacitive loading, the lower the cavity resonant frequency. In other words, a capacitively loaded cavity has smaller size than the unloaded one with the same resonant frequency.

Meanwhile, the magnetic field distribution remains nearly the same as in the unloaded cavity (Fig. 2c). Hence, the current distribution in the metallic parts of the resonator is mostly unaffected and the power dissipation in the cavity does not change significantly in the presence of the loading. As a result, the unloaded Q-factor does not drop as strongly as the resonant frequency does [10]. This leaves room to design highly loaded LTCC cavities that are as small as lumped-element resonators (i.e. smaller than $\lambda_g/8$) but still exhibit a much higher unloaded Q-factor.

The Q-factor dependence on the SIW cavity size in plane is shown in Fig. 2d for LTCC-filled CLCs of different size a but with the same height ($H = 1.44$ mm). The graph presents results of electromagnetic simulations. Eventually, a miniaturized CLC with the size $a = \lambda_g/10$ is characterized by the unloaded Q-factor of about 150. This is at least 2 – 3 times higher than the Q-factor of lumped-element resonators. According to (1), a bandpass filter using such CLCs has the same degree of advantage in insertion loss over its lumped-element counterpart.

A high capacitive loading is needed for an efficient size reduction of an SIW cavity. On the other hand, the smaller CLC size, the larger the ratio of the second and first resonant frequencies (Fig. 2e). For the above-mentioned example ($a = \lambda_g/10$) the ratio f_{02}/f_{01} is not less than 5 whereas for an unloaded square cavity the ratio is equal to $\sqrt{5/2} \approx 1.58$. Hence, highly loaded cavities allow the design of filters with no spurious response over a wide frequency range.

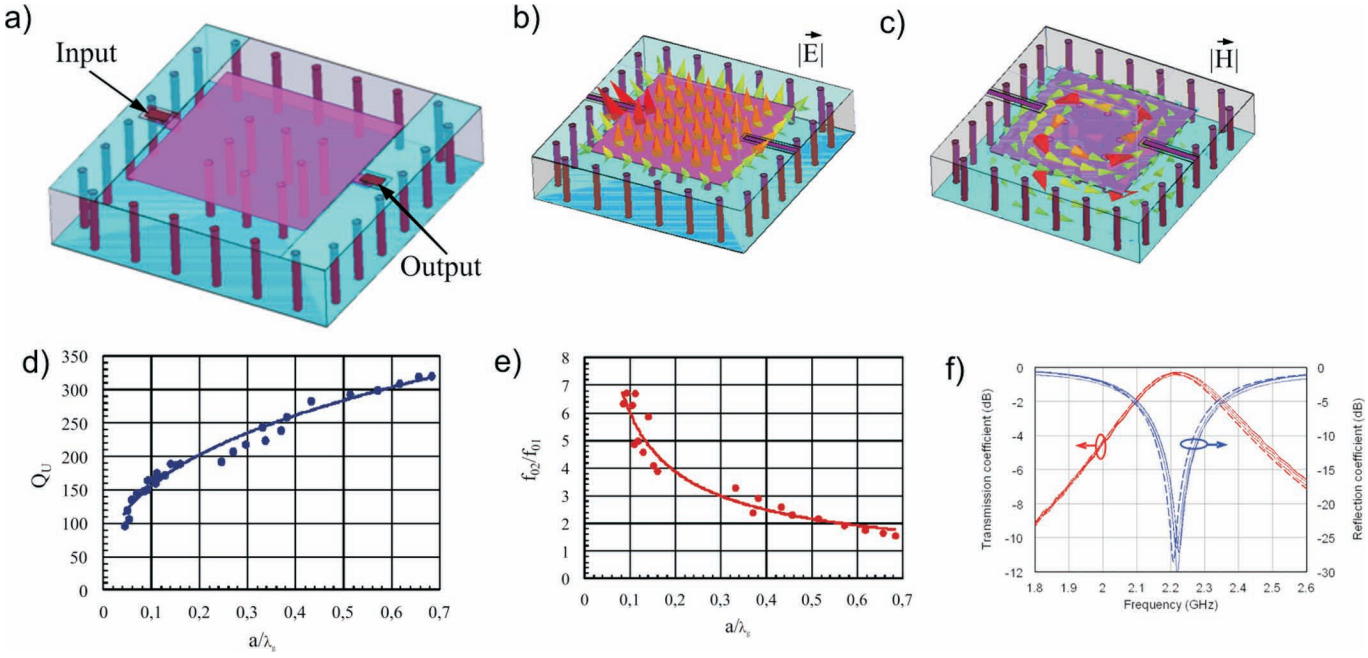

Fig. 2: Square-shape LTCC capacitively loaded cavity: (a) structure; (b) and (c) electric and magnetic field distribution for the fundamental mode; (d) unloaded Q-factor versus normalized cavity size; (e) second harmonic frequency versus normalized cavity size; (f) simulated characteristics of the resonator (dashed lines) and measured performance of four experimental samples (solid lines).

In practice, CLC size cannot be smaller than that of the metallic plate to realize the capacitive loading. In order to efficiently reduce the cavity size, the distance between the capacitive plate and the top cover should be minimized. For this purpose, the separating LTCC layer should be as thin as possible. However, it increases breakdown risk and consequently reduces power-handling capability. For LTCC materials, typical breakdown electric field strength is about 40 V/μm whereas the minimum layer thickness is limited to 40 – 50 μm. It allows power handling of a few Watt, which is sufficient for most portable electronics applications.

Fig. 2f presents the measured and simulated frequency responses of a CLC embedded in nine layers of DuPont Green Tape™ 951 LTCC ($\varepsilon_r = 7.8$, $\tan\delta = 0.002$) of different thickness. After sintering, six layers have the thickness of 210 μm, two layers are 42 μm thick, and one layer more has the thickness of 95 μm. Thus, the total height of the LTCC structure is about 1.44 mm. The internal size of the CLC with the resonant frequency of 2220 MHz is as small as 6 mm × 6 mm, corresponding to $\lambda_g/8$ size in plane. The conducting post measures 2 mm × 2 mm and is covered with the metallic plate measuring 4.4 mm × 4.4 mm. The resonator is connected to external circuits by inductive coupling elements as shown in Fig. 2a.

The CLC was manufactured using a standard LTCC technological process. DuPont 6148 Ag co-fireable conductor paste and DuPont 6141 AgPd co-fireable via fill paste were employed to realize the metallic parts of the resonator. A typical value of the conductive paste surface resistance ($R_{sur} = 5$ mΩ/square) was taken into account during the electromagnetic simulation with the Ansoft HFSS software

Experimental investigation was conducted using the Agilent PNA E8361 vector network analyzer and the Cascade Microtech Summit 9000 probe station with coplanar G-S-G probes for on-wafer measurements. The TRL technique was used for calibration.

A good repeatability of the measured frequency characteristics of four resonator experimental samples is observed (Fig. 2f). Besides this, the measured data agree well with the results of the electromagnetic simulation. The average unloaded Q-factor value extracted from the measured resonator characteristics is about 150.

At the resonant frequency, the resonator height $H = 1.44$ mm corresponds to $\lambda_g/32$. It is worth mentioning that the unloaded cavity of the same relative height is characterized not only by a significantly large area but also exhibits a much lower Q-factor (see, e.g. Fig. 1d).

(3) Coupled capacitively loaded cavities

CLCs can be coupled to each other in different ways.

As an example, an inter-resonator coupling can be organized by means of an iris in the mutual sidewall as shown in Fig. 3a. Although the nature of such a coupling is generally mixed (electric as well as magnetic), the main contribution comes from the electric field (i.e. capacitive coupling). The value of the coupling depends on the iris size *b*. The larger the iris size, the tighter the coupling. From this point of view, the cavity size *a* cannot be chosen fully arbitrarily as it should be sufficient to provide a required coupling value (i.e. $b \le a$).

The coupling coefficient *M* as a function of the iris size *b* related to the cavity size *a* is plotted in Fig. 3b. Measured and simulated frequency characteristics of a two-pole bandpass LTCC filter on a pair of iris-coupled CLCs are presented in comparison in Fig. 3c.

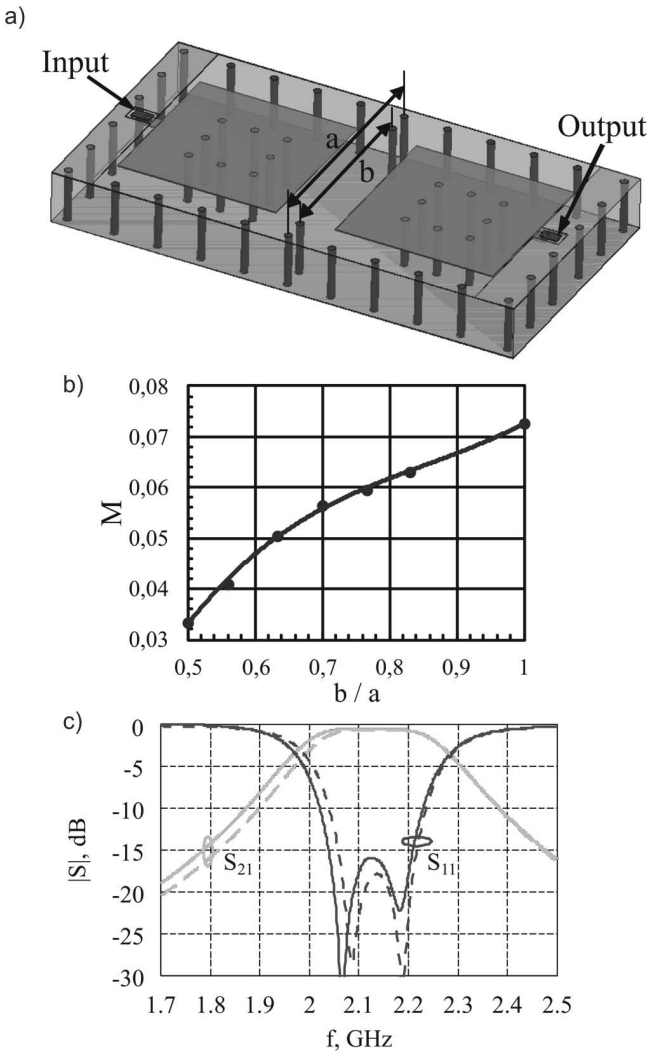

Fig. 3: Two-pole LTCC band pass filter on iris-coupled CLCs: (a) structure; (b) coupling coefficient as a function of the normalized iris size; (c) numerically simulated (dashed lines) and measured (solid lines) frequency response.

A different way to realize a capacitive coupling is to use a metal strip overlapping the capacitive plates of the two CLCs to be coupled. Such a coupling can be easily realized in multilayer technology.

The technique is efficient to realize weak couplings. It can be very helpful when the use of any iris leads to overcoupling. Besides, the technique can be used for fine adjustment of a via-iris coupling, e.g. in case of undercoupling.

As the metal strip to realize overlapping should go through a via fence which constitutes the mutual sidewall of the coupled CLCs, the strip width in this region is limited by a distance between adjacent metallic via holes. In order to provide the necessary coupling value, a dumbbell-shape strip (Fig. 4a) can be used. Coupling value is proportional to the overlapping area and inversely pro-

portional to the distance between the metal strip and the capacitive plates.

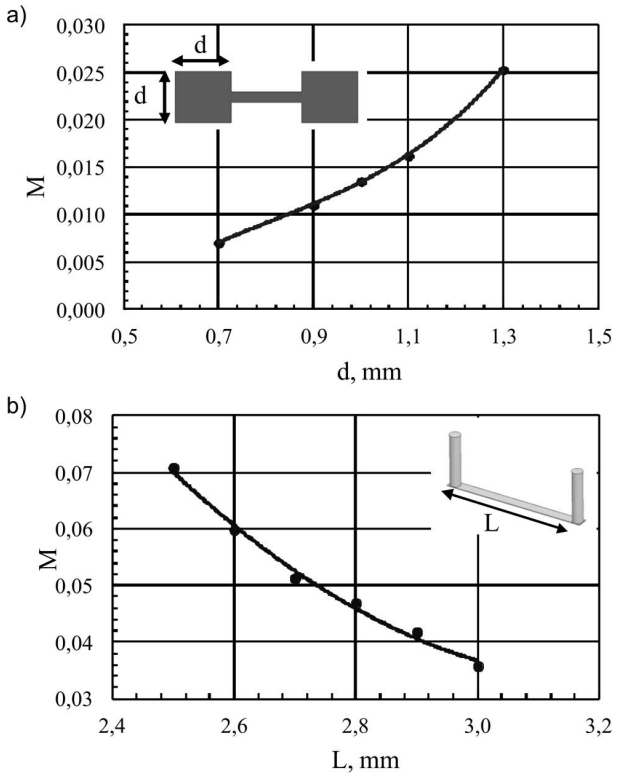

Fig. 4: Coupling coefficient versus geometrical parameter of the metal strip for capacitive (a) and inductive (b) couplings between CLCs.

An inductive coupling between two CLCs can be organized by using a narrow strip that is connected to the capacitive plates with the aid of metallic via holes (Fig. 4b) or directly when it is situated in the same metallization layer.

The coupling coefficient dependences on geometrical parameters of the metal strip for capacitive and inductive couplings (Figs. 4a and b) were obtained by means of electromagnetic simulation of a number of coupled CLC structures.

III. Advanced LTCC Bandpass Filters on CLCs

Design examples of small-size and low-loss bandpass LTCC filters on coupled CLCs are presented in this section.

(1) Three-pole filter

The multilayer LTCC structure of a three-pole bandpass LTCC filter on miniaturized CLCs is shown in Fig. 5a. The filter consists of three CLCs of the structure described in Section II(2). The inter-resonator couplings are organized by means of irises in the mutual sidewalls. In turn, the outermost CLCs are connected to external circuits by inductive coupling elements. The filter is embedded in nine layers of DuPont Green Tape™ 951 LTCC of different thickness (see section II(2) for details). The entire area occupied by the filter measures 19 mm × 7 mm ($0.38\lambda_g \times 0.14\lambda_g$).

The filter with the Chebyshev characteristic was designed for UMTS/LTE-2100 applications (2110 – 2170 MHz). An equivalent circuit of the filter is depicted in Fig. 5b.

Simulated and measured filter characteristics in the narrow and wide frequency ranges are presented in Fig. 5c. The in-band insertion loss does not exceed 1.2 dB, corresponding to the unloaded Q-factor of the CLCs equal to 150, i.e. at least three times higher than the Q-factor of quasi-lumped-element resonators. The CLC size is small enough compared to the wavelength that allows the filter to exhibit no spurious response up to at least 10 GHz (see Fig. 5c).

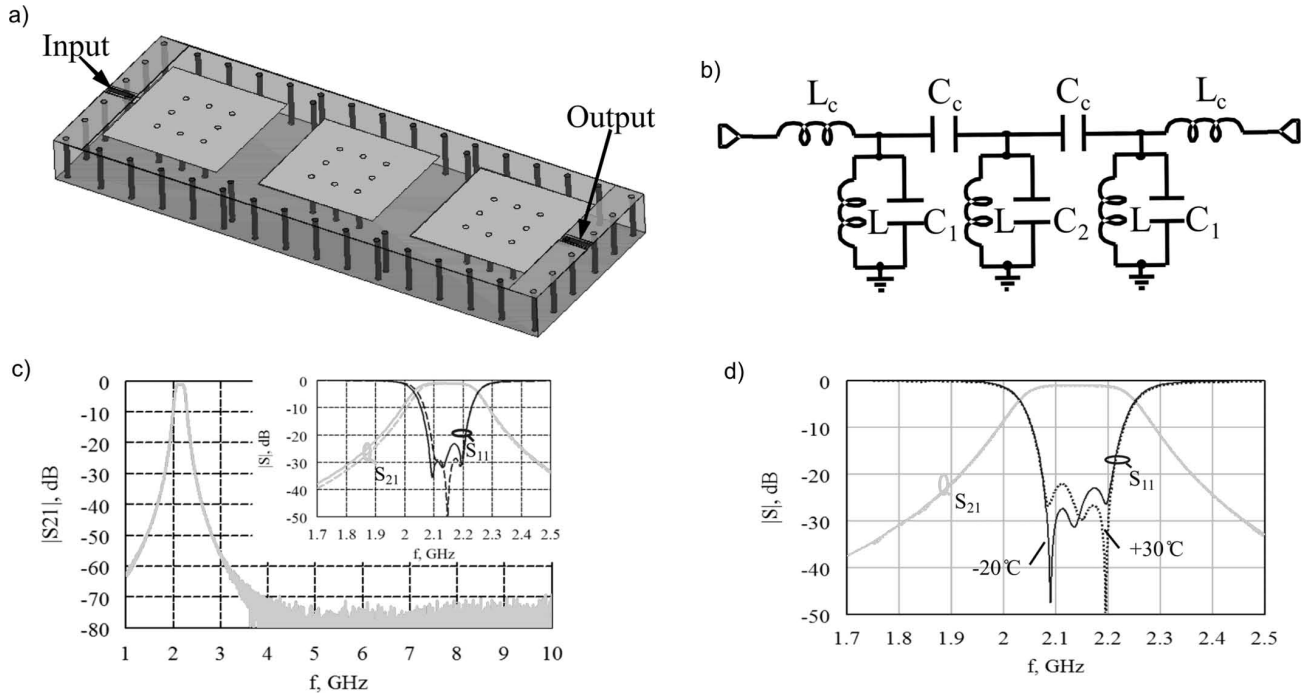

Fig. 5: Three-pole Chebyshev bandpass LTCC filter based on iris-coupled CLCs: (a) structure; (b) equivalent diagram; (c) measured (solid lines) and simulated (dashed lines) characteristics at room temperature; (d) measured characteristics under a temperature variation.

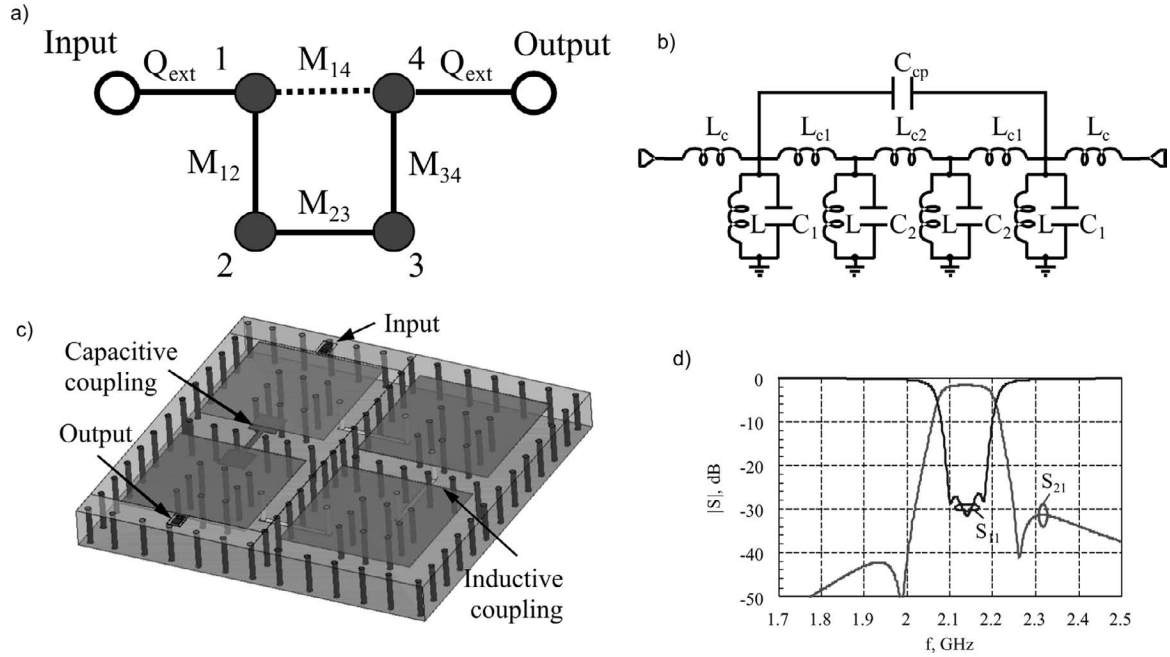

Fig. 6: Four-pole quasi-elliptic bandpass LTCC filter: (a) coupling scheme; (b) equivalent diagram; (c) structure; (d) frequency dependence of scattering parameters obtained by 3D electromagnetic simulation.

Fig. 5d shows the filter performance measured under the environmental temperature variation from −20 °C to +30 °C. The advanced CLC-based LTCC filter revealed good temperature stability of the frequency response within the specified temperature range.

(2) Four-pole cross-coupled filter

In order to improve selectivity, a four-pole bandpass filter with a cross coupling was designed for the same frequency band. The filter employs four CLCs of the same structure with three inductive couplings and a capacitive cross-coupling. The coupling scheme is shown in Fig. 6a. The matrix of the necessary coupling coefficient values is as follows:

$$M = \begin{pmatrix} 0.08 & 0.051 & 0 & -0.012 \\ 0.051 & 0 & 0.043 & 0 \\ 0 & 0.043 & 0 & 0.051 \\ -0.012 & 0 & 0.051 & 0.08 \end{pmatrix} \qquad (4).$$

Fig. 6b shows an equivalent circuit of the filter.

Three inductive couplings are formed by narrow metal strips connected to the capacitive plates of adjacent cavities. A capacitive cross-coupling between the outermost resonators is achieved with the aid of a dumbbell-shape metal strip overlaying the capacitive plate of the both coupled resonators. The multilayer LTCC structure of the filter is shown in Fig. 6c. The filter size in plane is 13 mm × 13 mm.

Simulated characteristics of the filter are presented in Fig. 6d. The bandpass filter with a cross-coupling provides two transmission zeros near the pass band edges that drastically increase the filter selectivity. The midband insertion loss of the filter equals to 1.7 dB.

IV. Bandpass Filters on Nested CLCs

(1) Capacitively loaded cavities with additional transmission zeros

A CLC can be surrounded by an extra metallic box in such a way that a space between the external CLC surface and the metallic box forms an additional capacitance C_z (Fig. 7a). An equivalent circuit of such a resonator is depicted in Fig. 7b. Presence of the capacitance C_z results in appearance of a transmission zero at the frequency

$$f_z = \frac{1}{2\pi\sqrt{L(C + C_z)}} \qquad (5).$$

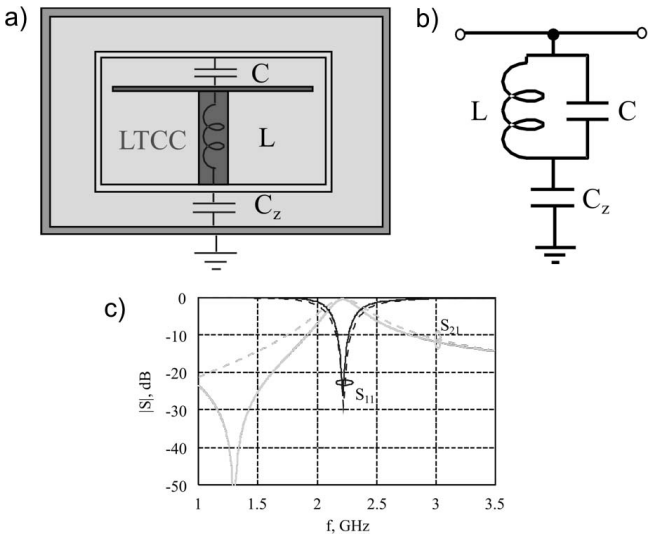

Fig. 7: CLC with a transmission zero: (a) schematic cross-sectional view (not to scale); (b) equivalent diagram; (c) simulated frequency response of the CLC with a transmission zero (solid lines) and without a transmission zero (dashed lines).

Frequency characteristics of the resonator with the resonant frequency $f_0 = 2.2$ GHz and a transmission zero at

$f_z = 1.3$ GHz are presented in Fig. 7c. For reference, the frequency response of CLC without a transmission zero is also plotted in the same graph.

CLCs with transmission zeros can be used to design small-size low-loss filters with enhanced selectivity. The approach does not require any cross-coupling to design filters with transmission zeros. In contrast to a cross-coupled filter structure involving four resonators (Figs. 6a, b, and c), the method under consideration can be applied to design, e.g. two-pole filters with transmission zeros. It allows an increase in filter selectivity at the expense of a very moderate increase of the occupied area and the structure height that is associated with the extra metallic box.

An example of a two-pole bandpass filter based on LTCC CLCs with transmission zeros is shown in Fig. 8a. The structure uses eleven layers of DuPont Green Tape™ 951 LTCC. The filter measures 14 mm × 8 mm × 1.9 mm in size. Fig. 8b illustrates an advantage in the selectivity of the filter with transmission zeros over a two-pole filter without transmission zeros.

(2) Dual-mode resonators on nested capacitively loaded cavities

CLCs with different resonant frequencies can be nested one into another like a set of the well-known traditional Russian dolls 'matryoshka' [15]. Fig. 9a illustrates a schematic cross-sectional view of two nested CLCs in LTCC. The external surface of the inner cavity acts as a capacitive loading for the outer cavity. It allows a reduction in the total area occupied by the two cavities. However, there is a trade-off between the occupied area reduction and an increase in height.

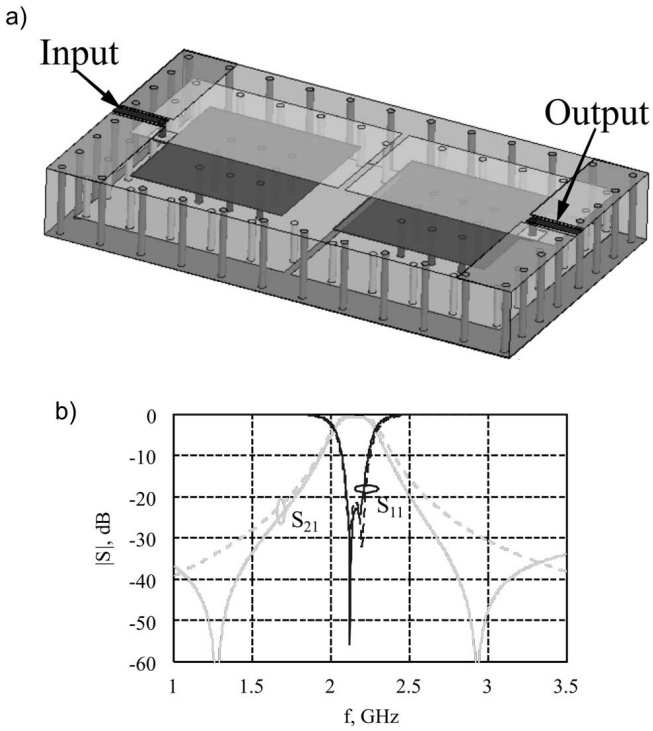

Fig. 8: Two-pole bandpass filter with transmission zeros: (a) LTCC structure; (b) simulated characteristics of the filter (solid lines) compared to those of a similar filter without transmission zeros (dashed lines).

The maximum height of LTCC structure is limited by the number and thickness of layers in a stack to be co-fired. The number of CLCs that can be nested one into another is therefore limited by technological facilities.

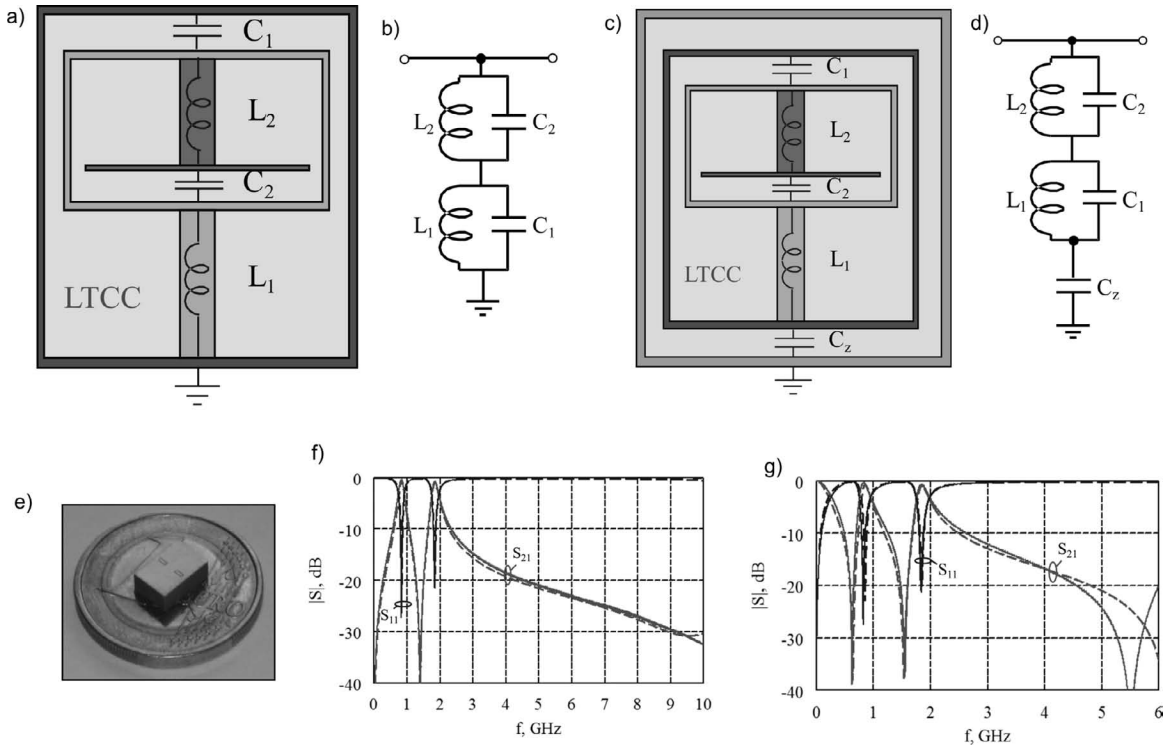

Fig. 9: Dual-mode LTCC resonators on nested CLCs: (a) and (b) schematic cross-sectional view and equivalent diagram of two nested CLCs; (c) and (d) schematic cross-sectional view and equivalent diagram of two nested CLCs providing an additional transmission zero; (e) photograph of a resonator experimental sample; (f) and (g) measured (solid lines) and simulated (dashed lines) characteristics of the dual-mode resonators without and with an additional transmission zero, correspondingly.

The two nested CLCs shown in Fig. 9a operate as a dual-mode resonator having two resonant frequencies which can be chosen almost arbitrarily, and provide a transmission zero between the two resonances. An equivalent circuit of such a dual-mode resonator consists of two parallel tanks connected in series as shown in Fig. 9b.

Similar to a single CLC, nested CLCs can be also surrounded by an extra metallic box to form an additional capacitance resulting in a transmission zero. A cross-sectional view and an equivalent circuit of the dual-mode resonator with a transmission zero on nested CLCs are shown in Figs. 9c and d respectively.

The frequency behavior of the dual-mode resonators on nested CLCs (with and without an additional transmission zero) was investigated with numerical electromagnetic simulations and experimentally. Test structures of the dual-mode resonators with as non-multiple resonant frequencies as f_{01} = 748 MHz and f_{02} = 1748 MHz were realized using sixteen layers of DuPont Green Tape™ 951 LTCC. A photograph of a resonator experimental sample is shown in Fig. 9e. The resonator structure size in plane is 7.6 mm × 5.2 mm, which does not exceed $\lambda_g/18$ at f_{01} and $\lambda_g/8$ at f_{02}. The height of the LTCC structure is 2.9 mm. Figs. 9f and -g present experimental characteristics of four tested samples of the dual-mode resonators with and without an additional transmission zero compared with those predicted by electromagnetic simulations. Good repeatability is observed for different samples as well as a good agreement between measured and simulated data.

Advantages of the dual-mode resonators on nested CLCs are as follows: i) resonant frequencies can be chosen almost arbitrarily; ii) less occupied area compared with two single-mode cavities; iii) still quite high Q-factor; iv) a transmission zero between the resonant frequencies; v) an additional transmission zero can be easily introduced; vi) no spurious response over a wide frequency range. The resonators are well suited for the design of miniature low-loss LTCC filters for dual-band applications.

(3) Dual-bandpass filters on nested capacitively loaded cavities

A structure of coupled dual-mode resonators based on two nested CLCs is shown schematically in Fig. 10a. The outer cavities are coupled to each other through an iris in the mutual sidewall. Additional irises in the adjacent sidewalls of the inner cavities are used to provide a coupling between them.

An equivalent diagram of the coupled resonators is presented in Fig. 10b. The coupling between the tanks with the resonant frequencies f_{01} and $f_{02} > f_{01}$ is represented by the capacitances C_{c1} and C_{c2} of different branches of the circuit. At the frequency f_{01} the two coupling capacitances get connected in parallel, so the total capacitance of the coupling is $C_c(f_{01}) = C_{c1} + C_{c2}$. Meanwhile, at f_{02} the coupling capacitance is $C_c(f_{02}) = C_{c2}$.

A design technique for dual-bandpass filters based on iris-coupled nested CLCs was proposed in [16]. As the first step, two single-band filters with the central frequencies f_{01} and f_{02} are designed separately using a conventional synthesis method. Then the coupling values of the filter designed for f_{01} are corrected as $C'_{c1} = C_{c1} - C_{c2}$. After this, the two filters are combined as shown in Fig. 10b. The technique allows the design of dual-band filters based on the CLC structures shown in Figs. 9a and c.

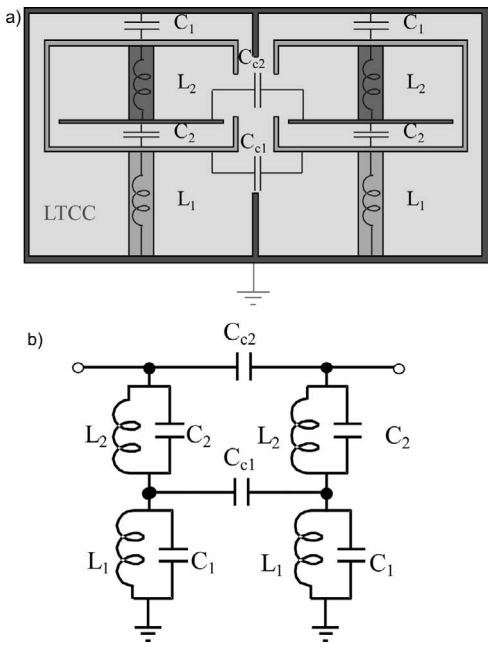

Fig. 10: Coupled dual-mode resonators based on nested CLCs: (a) schematic cross-sectional view; (b) equivalent diagram.

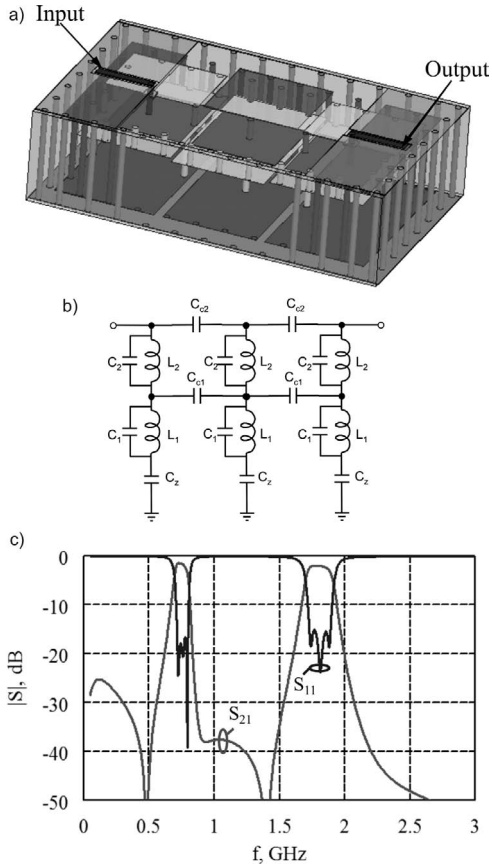

Fig. 11: Three-pole dual-bandpass LTCC filter on nested CLCs: (a) structure; (b) equivalent diagram; (c) characteristics obtained by a full-wave numerical simulation.

A design example of the three-pole dual-band filter with the pass bands of 698–798 MHz and 1710–1788 MHz is shown in Fig. 11. The filter was realized in LTCC

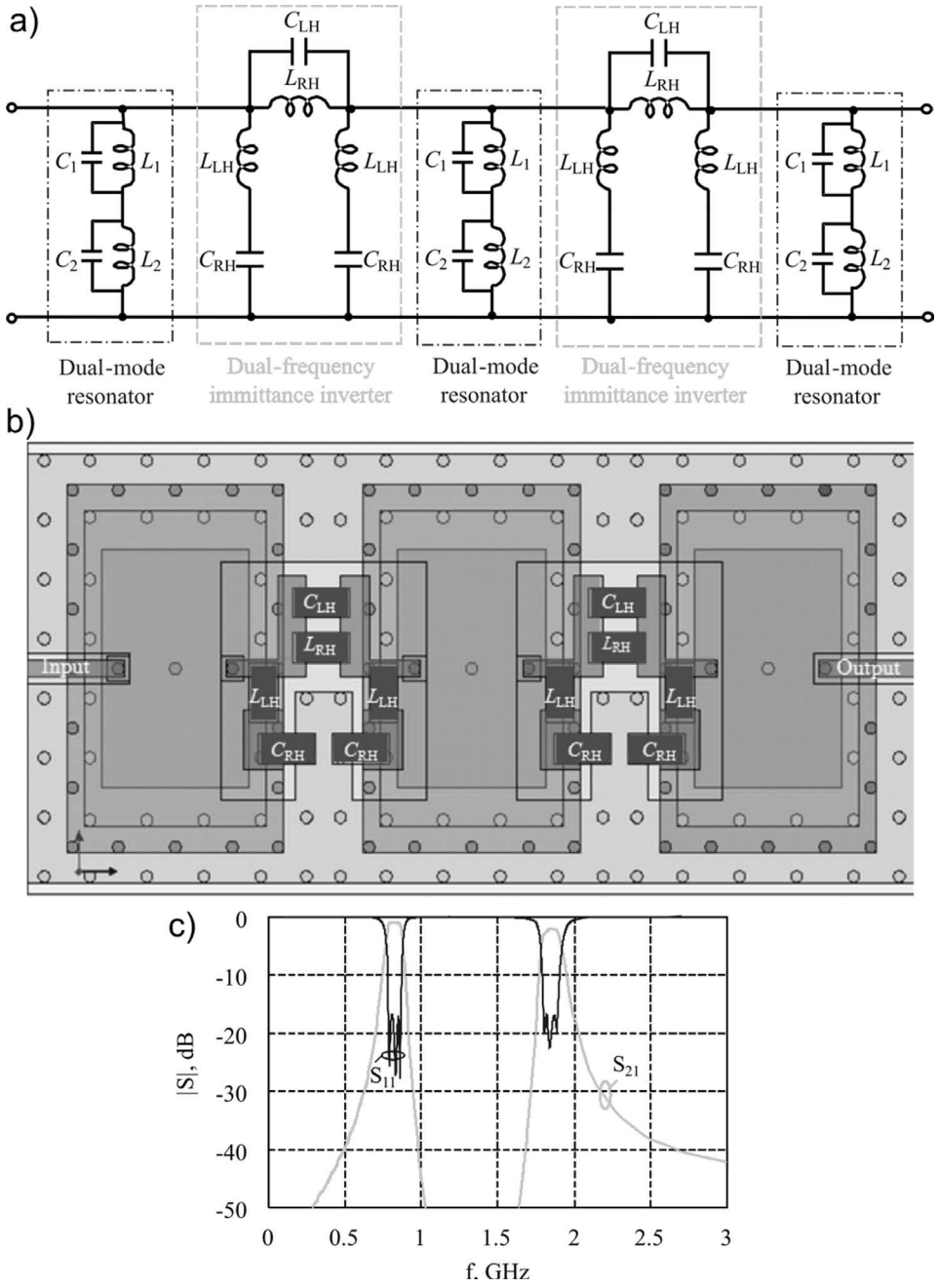

Fig. 12: Three-pole dual-bandpass LTCC filter on nested CLCs with lumped-element dual-frequency immittance inverters: (a) equivalent diagram; (b) top-view of LTCC structure; (c) characteristics obtained by a full-wave numerical simulation.

technology using the above-mentioned structure of the dual-mode resonator (Fig. 9c). The filter is as small as 12 mm × 7.6 mm, corresponding to only $\lambda_g/12$. It provides a low insertion loss (1.4 dB and 2.1 dB in the lower and higher pass bands, respectively) and a high selectivity.

Besides rather sophisticated iris couplings between the dual-mode resonators on nested CLCs, dual-bandpass filters based on such resonators can also employ dual-frequency immittance inverters on lumped elements [17–19]. Fig. 12 shows an example of a three-pole filter design using such immittance inverters. Three dual-mode nested CLCs are embedded in a single LTCC structure similar to the previous case. The dual-frequency immittance inverters (see Fig. 12a) are realized on lumped elements which are surface mounted on the top of the LTCC structure as illustrated in Fig. 12b. A simulated filter performance is presented in Fig. 12c. Owing to a specific frequency response of the dual-frequency immittance inverters involved [17–19], the filter provides an increased rejection between the pass bands compared to the design shown in Fig. 11.

V. Conclusion

Design of high-performance microwave bandpass filters requires the use of high-Q miniaturized resonators. A trade-off between resonator size and Q-factor value makes the design of small-size and low-loss filters a challenge. Cavity resonators are of high Q-factor but have a significant size. In turn, lumped-element resonators are very compact but characterized by a poor Q-factor.

Capacitively loaded SIW cavities can be considered a promising solution. The higher the capacitive loading, the lower the cavity size for a given resonant frequency. The Q-factor also decreases with a capacitive loading increase. However, due to a specific electromagnetic field distribution in the CLC, the Q-factor does not change as remarkably as the resonator size does. This leaves room to design miniaturized CLCs with a relatively high unloaded Q-factor.

Multilayer LTCC technology is well suited to realize miniaturized resonators based on SIW cavities with a high capacitive loading. It offers manifold possibilities and high flexibility to realize single- and multi-mode CLCs with and without transmission zeros.

It was demonstrated by the results of numerical electromagnetic simulations and experimental investigations that highly loaded LTCC cavities operating in the TM_{110} mode can be smaller than $\lambda_g/8$, i.e. comparable in size with lumped element resonators while exhibiting a much higher unloaded Q-factor.

The miniaturized LTCC-based CLCs were shown as advantageous for the design of small-size and low-loss bandpass filters with no spurious response over a wide frequency range.

Various examples of the advanced LTCC resonators and filters designed for wireless communication frequency bands were presented. All the devices were manufactured on the commercial DuPont Green Tape™ 951 LTCC system in a standard technological process.

The experimental investigations of the designed high-performance resonators and filters revealed that a typical manufacturing accuracy of LTCC structures is sufficient to provide a good repeatability of the frequency characteristics for a number of experimental samples of the resonators and filters as well as good agreement between the measured frequency responses and those predicted based on electromagnetic simulations.

Acknowledgement

The work was supported by the German Research Foundation (DFG) within the framework of the MACRAME (HE 3642/8 – 1) project and by the Ministry for Education and Science of the Russian Federation under the Project State Assignment No. 8.1825.2014/K.

References

1 Bozzi, M., Georgiadis, M.A., Wu, K.: Review of substrate-integrated waveguide circuits and antennas, *IET Microw. Antenna P.*, **5**, [8], 909 – 920, (2011).

2 Lee, J.-H., Pinel, S., Papapolymerou, J., Laskar, J., Tentzeris, M.M.: Low loss LTCC cavity filters using system-on-package technology at 60 GHz, *IEEE T. Microw. Theory*, **53**, [12], 3817 – 3824, (2005).

3 Potelon, B., Bohorquez, J.-C., Favennec, J.-F., Quendo, C., Rius, E., Person, C.: Design of Ku-band filter based on substrate-integrated circular cavities (SICCs). In: 2006 IEEE MTT-S Int. Microw. Symp. Dig. San Francisco, California, 1237 – 1240, (2006).

4 Shen, T.-M., Chen, C.-F., Huang, T.-Y., Wu, R.-B.: Design of vertically stacked waveguide filters in LTCC, *IEEE T. Microw. Theory*, **55**, [8], 1771 – 1779, (2007).

5 Zhang, X.-C., Yu, Z.-Y., Xu, J.: Novel band-pass substrate integrated waveguide (SIW) filter based on complementary split ring resonators (CSRRS), *Prog. Electromagn. Res.*, **72**, 39 – 46, (2007).

6 Potelon, B., Favennec, J.-F., Quendo, C., Rius, E., Person, C., Bohorquez, J.-C.: Design of a substrate integrated waveguide (SIW) filter using a novel topology of coupling, *IEEE Microw. Wirel. Co.*, **18**, [9], 596 – 598, (2008).

7 Tsai, W.-L., Wu, R.-B.: Tri-band filter design using substrate integrated waveguide resonators in LTCC. In: 2010 IEEE MTT-S Int. Microw. Symp. Dig. Anaheim, California, 445 – 448, (2010).

8 Xu, Z.Q., Shi, Y., Wang, P., Liao, J.X., Wei, X.B.: Substrate integrated waveguide (SIW) filter with hexagonal resonator, *J. Electromagnet. Wave*, **26**, [11 – 12], 1521 – 1527, (2012).

9 Xu, L.-J., Wang, J.P., Guo, Y.-X., Wu, W.: Double-folded substrate integrated waveguide band-pass filter with transmission zeros in LTCC, *J. Electromagnet Wave.*, **27**, [1], 96 – 103, (2013).

10 Gong, X., Margomenos, A., Liu, B., Chappell, W.J., Katehi, L.P.B.: High-Q evanescent-mode filters using silicon micromachining and polymer stereolithography (SL) processing. In: 2004 IEEE MTT-S Int. Microw. Symp. Dig. Fort Worth, Texas, 433 – 436, (2004).

11 Ferrand, P., Baillargeat, D., Verdeyme, S., Puech, J., Lahti, M., Jaakola, T.: LTCC reduced-size bandpass filters based on capacitively loaded cavities for Q-band application, In: 2005 IEEE MTT-S Int. Microw. Symp. Dig. Long Beach, California, 1789 – 1792, (2005).

12 Rigaudeau, L., Ferrand, P., Baillargeat, D., Bila, S., Verdeyme, S., Lahti, M., Jaakola, T.: LTCC 3-D resonators applied to the design of very compact filters for Q-band applications, *IEEE T. Microw. Theory*, **54**, [6], 2620 – 2627, (2006).

13 Joshi, H., Sigmarsson, H.H., Peroulis, D., Chappell, W.J.: Highly loaded evanescent cavities for widely tunable high-Q filters. In: 2007 IEEE MTT-S Int. Microw. Symp. Dig. Honolulu, Hawaii, 2133 – 2136, (2007).

14 Kushta, T., Harada, T.: New 3-D design of filtering components using multilayer board technologies. In: Proc. 38th Eur. Microw. Conf., Amsterdam, the Netherlands, 218 – 221, (2008).

15 Turgaliev, V., Kholodnyak, D., Vendik, I., Stöpel, D., Humbla, S., Müller, J., Hein, M.A.: LTCC highly loaded cavities for the design of single- and dual-band low-loss miniature filters. In: Proc. 40th Eur. Microw. Conf., Paris, France, pp. 180 – 183, (2010).

16 Turgaliev, V., Kholodnyak D., Vendik, I.: Small-size dual-band filters on capacitively loaded cavities. In: Proc. 43rd Eur. Microw. Conf., Nuremberg, Germany, 660 – 663, (2013).

17 Kholodnyak, D.V., Turalchuk, P.A., Zameshaeva, E. Yu.: Dual-frequency immittance inverter with a stop-band between the operation frequencies based on one-dimensional metamaterials. Patent RU 2463690 C2, (2012), (in Russian).

18 Kholodnyak, D., Turgaliev, V., Vorobev, E.: Advanced microwave filters in LTCC and PCB technologies. In: Proc. 2014 Asia-Pacific Microw. Conf., Sendai, Japan, 88 – 90, (2014).

19 Kholodnyak, D., Turgaliev, V., Zameshaeva, E.: Dual-band immittance inverters on dual-composite right/left-handed transmission line (D-CRLH TL). In: Proc. 9th German Microw. Conf., Nuremberg, Germany, 60 – 63, (2015).